

Simulation and Measurement Results of 150 GHz Integrated Silicon IMPATT Diodes

Manuel Luschas¹, Rolf Judaschke¹, Johann-Friedrich Luy²

¹ Arbeitsbereich Hochfrequenztechnik, TU Hamburg-Harburg, Germany

² DaimlerChrysler Research Center, FT2/HM, Ulm, Germany

Abstract — The integration of IMPATT diodes and their housing in a single technology process is discussed in this paper. The integrated device is designed to improve reliability and reproducibility compared to conventional beam-lead diodes with quartz ring housing. In a single step, the diode with its housing is bonded onto a diamond heat sink. The device can be employed both in a waveguide resonator and in a planar oscillator circuit. Results presented here are obtained in a rectangular, reduced height waveguide resonator. RF-output power levels of more than 100 mW at 135 GHz and 45 mW at 150 GHz are reported.

I. INTRODUCTION

IMPATT diodes are to date the only semiconductor source of high RF-output power above 100 GHz. However, they are often used with reluctance because of tuning difficulties in an RF-circuit. On the one hand, they are expensive because of the low production yield and, on the other hand, fragile to work with because they operate at their thermal limit. Conventional quartz ring diodes have varying electrical properties because of the large number of manual work steps in the fabrication process.

When manufacturing IMPATT diodes, there are two major concerns for yielding high RF-output power. The first issue is the design and realization of an optimal doping profile. The second challenge is to achieve reliable, low loss thermal and electrical contacts.

The doping profile of choice for high output power is the double low-high-low (DLHL) structure. The concentration of the high electric field in the avalanche region reduces the operating voltage compared to a flat double drift (DD) design. This improves efficiency since the device can be driven with a higher current density when DC-power dissipation is held constant.

Computer optimization of such a doping profile can be performed using a 1D-hydro-dynamic device simulator. Attention must be paid to the feasibility of the optimized design since the doping layer thickness might approach the minimum resolution of the molecular beam epitaxy (MBE).

To reduce the thermal resistance, special care must be taken when bonding diodes. Handling the diodes, which

typically have diameters of a few 10 μm , is tricky. Merging the fabrication of the active element with that of the housing in one technology process eliminates the need for several bonding steps during manufacturing. Fewer manual work steps results in better reliability, better reproducibility and faster, cheaper production of devices.

II. DIODE DESIGN

The design goal is to maximize the negative resistance of the active element in the D-band frequency range to maximize RF-output power.

The DC-current density which corresponds to the DC-power dissipation of the IMPATT diode is the limiting factor to achieving a large negative resistance. Thus, the operating voltage has to be minimized in order to maximize the DC-current through the diode.

The properties of the Si-MBE also need to be considered in the design. The spikes in the doping concentration and their width are close to the minimum resolution of the Si-MBE for a DLHL D-band IMPATT design.

Simulation and optimization of the doping profile are carried out using an in-house hydro-dynamic carrier transport model based simulator [1]. According to [1] the doping profile has been optimized at a DC-current of 250 mA and an RF-voltage of 5 V at an operating temperature of 500 K. Figure 5 compares simulation and measurement results of the diodes' output power.

Simulation results show that a breakdown voltage as low as 8.5 V and theoretical RF-output power values between 200–250 mW in the D-band range can be achieved. The actual MBE-grown doping profile was measured in the center of the 4" wafer by the secondary ion mass spectroscopy (SIMS) analysis. The optimized and measured doping profiles with their resulting electric fields under DC-bias condition are shown in Figure 1. The accuracy of the MBE is within the typical specification of an integral error in the doping concentration of up to 25%, except for the doping concentration of the p-drift region, where it is off by 80%.

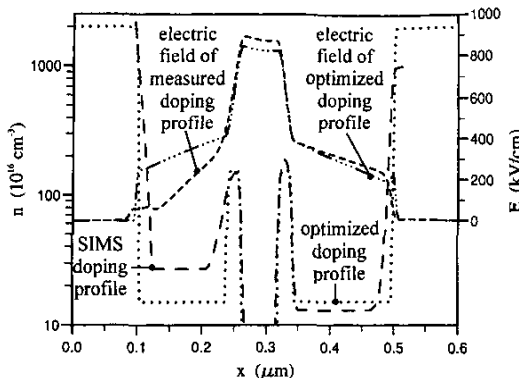


Fig. 1. Simulated electric fields and doping profiles of the optimized and of the SIMS-analyzed MBE-grown DLHL-IMPATT diode.

This results in a reduction of the electric field below the saturated carrier drift velocity threshold. The large deviation from the desired doping concentration is due to the difficulties in calibrating the Boron donation of the MBE when growing a profile on a wafer with a buried isolation layer.

Superior output power results cannot be expected from such a doping profile. Nevertheless, the goal of the present work is to demonstrate the feasibility and operation of the novel device integration concept.

III. TECHNOLOGY PROCESS

Reference [2] reports the integration of IMPATT diode and housing in a single device for GaAs technology. Here, the realization of the process in Si technology will be described. The work is motivated by the fact that the published output power of Si-IMPATT diodes at D-band frequencies are superior to those made of GaAs [2, 3, 4].

The introduced technology process is a further development of an existing beam-lead diode process [4].

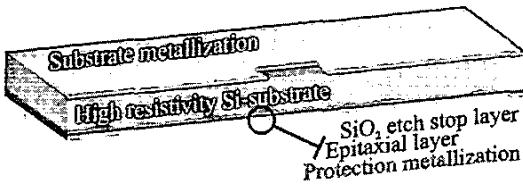


Fig. 2. Cross-section view of the SIMOX wafer before via hole etching.

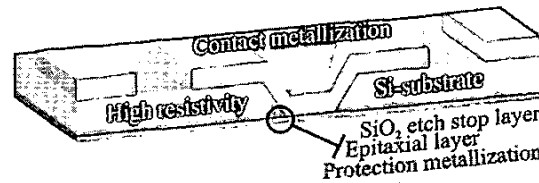


Fig. 3. Cross-section view of the electroplated via hole.

First, the active layer is grown by MBE on a 4" high resistivity SIMOX (Separation by Implanted Oxygen) wafer. The buried oxide layer is used both as etch stop and isolation layer between the upper and the lower contacts.

The wafer is then thinned to a thickness of 30 μm , which is the chosen device height. The active layer has to be contacted from the substrate side. Figure 2 shows the lithographically structured Ti/Au-metallization on the substrate side. This metallization is used as an etch mask.

In a wet chemical etch step, a via hole is etched with hot, aqueous KOH. The etching process is stopped at the oxide layer just above the active layer because of the high etching selectivity for Si and SiO_2 . In a dry etch step, the SiO_2 is removed and the via hole is extended into the oversized n'-contact layer of the DLHL diode structure.

The top contact is realized by evaporating a Ti/Au-metallization on the substrate side into the via hole. The metallization is lithographically structured and electroplated to a thickness of about 15 μm . This thick metallization is needed to guarantee a good bond contact, since the mesa diode is attached only to the gold layer at the bottom of the via hole. The bonding pressure that the diode experiences is determined by the thickness of the metallization. The processed substrate side of the wafer is depicted in Figure 3.

On the epitaxial side of the wafer, mesa and stand-off structures are defined by plasma etching using the lithographically structured contact metallization as an etch mask, see Figure 4. The stand-off seals the mesa diode hermetically from the environment and prevents any exposure to mechanical stress.

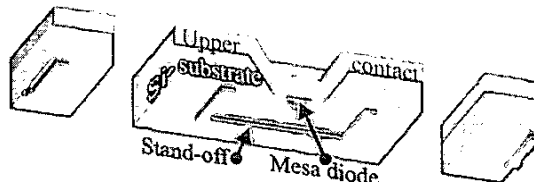


Fig. 4. Cross-section view of the back side of a processed, integrated Si-IMPATT device.

Finally, the devices are separated in a dry etch step. A SEM picture of a processed diode device is shown in Figure 5. Its dimensions are $200 \times 200 \mu\text{m}^2$ with a height of $45 \mu\text{m}$. A binary coding with cut-off corners is used to easily determine the diameter of the mesa diode on the back side of the device.

IV. DEVICE BONDING

The primary advantage of the device concept becomes clear after device processing. The bonding of the devices is less time consuming and much easier to handle compared to the bonding of conventional beam-lead quartz ring diodes. A few tests are sufficient for finding the optimal bond pressure, temperature and time to ensure good bond quality.

A flat bondhead is used to thermocompression-bond the device onto a diamond heat sink. No adjustments of the diode chip itself are needed. The thermal resistance characterizes the quality of the bond contact. A measurement technique for the thermal resistance is introduced in [5]. Measurements show typical values of the thermal resistance in the range of $50 - 60 \text{ K/W}$.

Typical values of the thermal resistance for beam-lead diode bonds are in the range of $70 - 80 \text{ K/W}$. For all measurements a general temperature drift coefficient of the breakdown voltage $\beta \sim 0.0008$ was used instead of individually measured values. Qualitatively, it can be concluded that the bond quality has been improved in the present device technology. The device can be driven with a higher current density and can thus generate higher RF-output power.

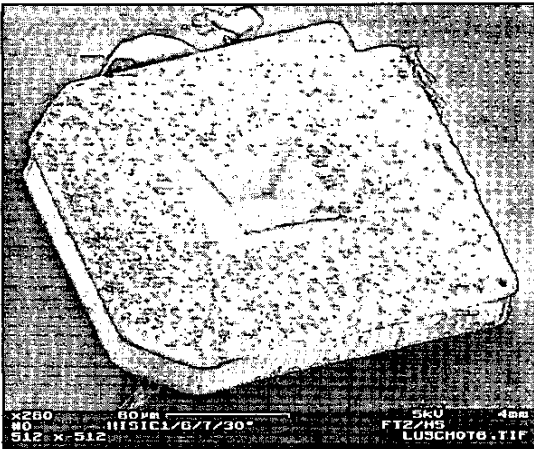


Fig. 5. SEM-picture of a top view of an integrated Si-IMPATT device.

V. MEASUREMENTS

Simulation results show that the electrical properties of the integrated devices are similar to those of the quartz ring diodes [4]. Thus, the same oscillator setup, i. e. a reduced height rectangular waveguide mount with a sliding short, is used for RF-characterization.

In the waveguide resonator setup, the diode height relative to the waveguide is adjusted with a micrometer-drive. The device is contacted with an RF-choke from the opposite side of the waveguide. A thin metal disk is placed on top of the active device to match the waveguide and the diode impedance. Frequency tuning is possible with disks of different diameter. Typical in the range of $140 - 150 \text{ GHz}$ are disks with $0.7 - 0.8 \text{ mm}$ diameter.

Shown in Figure 6 are the measured output power values of the integrated devices in the waveguide resonator setup. To compare these numbers to the theoretically achievable values, simulation results of the measured diode doping structure are depicted. Additional simulation results accounting for the previously neglected series resistance losses are also shown. These results explain the low measured RF-output power values.

Remarkably, the RF output power at 150 GHz is reduced by over 3 dB when a series resistance of 1Ω is included and by almost 10 dB with a series resistance of 1.5Ω . DC-characterization of the devices under test show series resistances above 1.5Ω . Taking this into account, good agreement of the measured and calculated values can be observed.

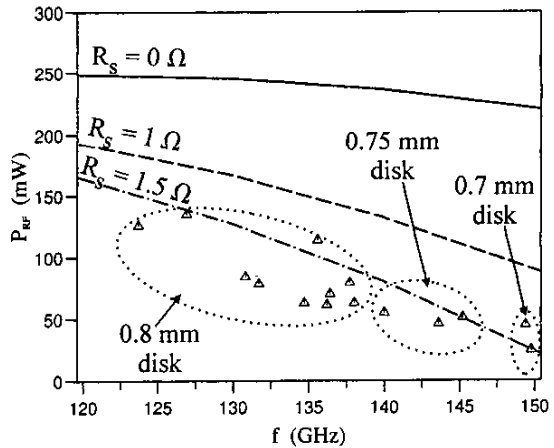


Fig. 6. Simulated and measured RF-output power of integrated IMPATT diodes; simulation results for 0Ω , 1Ω and 1.5Ω series resistance, measured results for different disk diameters; parameters: $I_0=250 \text{ mA}$, $U_b=5 \text{ V}$, $T=500 \text{ K}$, $d=23 \mu\text{m}$.

Nevertheless, the series resistance has to be reduced to values under 1Ω , which is a typical value for beam-lead diodes. This can be accomplished by ensuring better accuracy in the etch steps when contacting the active layer during the technology process.

Note that series resistances are due to processing imperfections, while thermal resistances are due to bonding or metallization imperfections.

Diode test parameters are set to match the simulation results. The DC-current is 250 mA and diode diameters are about 23 μm . In the region of 135 GHz, an RF-output power of over 100 mW can be reported. Values of 60 mW and 45 mW were achieved at 145 GHz and 150 GHz, respectively. The results at 150 GHz and 145 GHz are obtained using a 0.7 mm and 0.75 mm disks, respectively. Below this frequency range, 0.8 mm disks were used as matching elements in the RF-circuit.

VI. CONCLUSION

The realization of packaged Si-IMPATT diodes for the D-band frequency range is described. The introduced technology process integrates the active diode chip with its housing, resulting in easier fabrication and higher device reliability. Multiple bonding steps and manual adjustments of μm -sized parts that are necessary when manufacturing beam-lead diodes are reduced to one bonding step of a relatively large, integrated device.

Simulation results of the computer optimized DLHL doping profile as well as the actual manufactured doping profile are presented to explain the relatively low RF-output power of the new devices. RF-measurements show peak output power values of over 100 mW at 135 GHz and 45 mW at 150 GHz with a DC-current of 250 mA and a diode diameter of 23 μm . DC-measurements of the fabricated devices compared to the simulated data show a high series resistance of 1.5Ω .

Future work should concentrate on the reduction of series resistance to values achieved with beam-lead diodes, and a more accurate realization of the optimized doping profile with the MBE. This would result in RF-output power levels comparable to conventional beam-lead diodes.

ACKNOWLEDGEMENT

This work has been performed at the DaimlerChrysler Research Center, FT2/HM, Ulm, Germany, in cooperation with the Arbeitsbereich Hochfrequenztechnik of the Technische Universität Hamburg-Harburg, Germany. It is part of the Deutsche Forschungsgemeinschaft Forschergruppe "Submillimeterwellen-Schaltungstechnologie". The authors are indebted to the Deutsche Forschungsgemeinschaft for financial support.

REFERENCES

- [1] M. Curow, *Konsistente Simulation von Millimeterwellen-Oszillatoren mit Gunn-Elementen und IMPATT-Dioden*, Technische Universität Hamburg-Harburg, Hamburg, 1996.
- [2] M. Tschermitz, *Optimierung von GaAs-Lawinenlaufzeitdioden mit Hilfe einer neuartigen monolithischen Einbautechnik*, Lehrstuhl für allgemeine Elektrotechnik und angewandte Elektrotechnik der Technischen Universität München, München, 1995.
- [3] M. Wollitzer, J. Büchler, F. Schäffler, J.-F. Luy, "D-band Si-IMPATT diodes with 300 mW CW output power at 140 GHz," *Electronic Letters*, 32, pp. 122 - 123, Feb. 1996.
- [4] M. Wollitzer, *Planare Silizium-IMPATT-Oszillatorschaltungen bei 140 GHz*, Fortschritt-Berichte VDI, Nr. 286, ISBN 3-18-328609-2, 1998.
- [5] R. H. Haitz, H. L. Stover, N. J. Tolar, "A Method for Heat Flow Resistance Measurements in Avalanche Diodes," *IEEE Trans. Electron Devices*, Vol. ED-16, No. 5, 438-444, May 1969.